Research Article GU J Sci 35(2): 372-386 (2022) DOI: 10.35378/gujs.843764

Gazi University

Journal of Science

http://dergipark.gov.tr/gujs

Carbon Dioxide Capture Properties of $MgCl_2$ Templated Microporous Carbon from p-toluenesulfonic Acid

Ali Can ZAMAN*

Science and Technology Application and Research Center, Yıldız Technical University, Esenler, 34200, Istanbul, Turkey

Highlights

- Toluenesulfonic acid is used to produce porous carbons for CO_2 capture.
- $MgCl_2.6H_2O$ is used as template.
- $MgCl_2$ templating does not enhance ultramicroporosity development.

Article Info

Received:20 Dec 2020
Accepted:9 June 2021

Keywords

CO_2 capture
Microporous carbon
Sulfur doped carbon
Physisorption

Abstract

Herein, porous carbon materials were prepared using p-toluenesulfonic acid (TsOH) as a carbon source with (TsOH-STC) and without (TsOH-C) presence of $MgCl_2.6H_2O$. The products were evaluated in terms of CO_2 (carbon dioxide) adsorption performance, texture and surface chemical structure. Both samples contain oxidized sulfur on their surface according to X-ray photoelectron spectroscopy (XPS). TsOH-STC has a 3D porous network, but TsOH-C consists of a dense structure. It was understood that TsOH-C is not suitable to be analyzed with N_2 adsorption at cryogenic temperatures probably due to restricted access to narrow pores due to lack of external surface. The CO_2 uptakes are 0.78 mmol g^{-1} for TsOH-C and 0.67 mmol g^{-1} for TsOH-STC at flue gas conditions (0.15 bar and 298 K) of coal fired power plants, which is a projection of ultramicropore (pores smaller than 0.7 nm) volume in 0.5 nm range. TsOH-C has CO_2 uptake capacity of 2.21 mmol g^{-1} and TsOH-STC reaches 2.47 mmol g^{-1} at 1 bar at 298 K. Maximum CO_2 adsorption enthalpy (Q_{st}) value for TsOH-C is 24.9 kJ mol^{-1} and that of TsOH-STC is 25.7 kJ mol^{-1}. IAST (ideal adsorbed solution theory) selectivities (CO_2:N_2 = 15:85) of the samples are 13.5 for TsOH-STC and 19.7 for TsOH-C at 1 bar. It was shown in this study that salt templating with $MgCl_2$ does not influence ultramicroporosity development and provide moderate level CO_2 capture performance. However, templating induces formation of supermicropores (micropores larger than 0.7 nm), large mesopores and macropores on TsOH derived carbons.

1. INTRODUCTION

CO_2 (carbon dioxide) is a greenhouse gas, which is the major concern for the global warming [1]. CO_2 is a byproduct of fossil fuel combustion [1]. Post-combustion CO_2 capture method is the simplest method to capture released CO_2 from coal-fired power plants [2]. Membrane, cryogenic, adsorption by chemical solvents and solid adsorbents were developed for CO_2 capture [3]. The flue gas is adsorbed using amine solutions (chemisorption by solvents) conventionally [4]. However, the technology relies on toxic chemicals and contaminant by-products [5] and high regeneration cost [6]. Among the exemplified CO_2 capture technologies adsorption by solid adsorbents technology holds promise because of its low cost and simplicity. MOFs, zeolites, carbons, and porous organic polymers can be used as solid adsorbents [3]. Porous carbons particularly find use in catalysis and adsorption applications [7], and they are good candidates to be used for CO_2 adsoption because of their suitability to be utilized in post-combustion CO_2 capture, which is carried out at atmospheric pressure (1 bar), and at low concentration of CO_2 (0.15 bar) [8]. There are many aspects needed to be considered for a successful carbon adsorbent, which are appropriate pore structure and sufficient chemical interaction for easy regeneration and high gas selectivity. It is possible to produce carbons from suitable carbonizable precursors by pyrolysis without the need for additives. Nevertheless, the produced carbons can`t acquire sufficient porosity. Hence, generally activation strategies are employed [9,10]. It can be chemical or physical depending on the activation type used.

*e-mail: aczaman@yildiz.edu.tr

Chemical activation with KOH impregnation and pyrolysis of the precursor-KOH mixture in inert atmosphere is the generally used activation strategy [11,12]. However, KOH is toxic. New strategies should be sought. Using templates to provide porosity in carbon materials can be a feasible strategy. Hard templating approach is one of those [13]. With appropriate salts additives, carbon acquires porosity replicating the salt crystal geometry. In addition, presence of salts may influence the surface chemical structure by inducing a catalytic effect. Appropriate salt-precursor combination may also be important for synergistic effect on porosity. So there is a need for investigating the properties of carbons synthesized with simple pyrolysis and salt templating methods. Besides, there is limited amount of study dealing with $MgCl_2$ templated carbons [14].

Nitrogen doped carbons are popular in the field of porous carbon production for CO_2 capture applications [15,16]. Nitrogen is popular because it renders the surface of carbon material basic. The carbon material which possesses basicity on its surface can have high adsoption capacity for CO_2, isosteric heat of adsorption and CO_2/N_2 gas selectivity. As in the case of nitrogen, sulfur may also provide acid-base interaction with CO_2 molecules [17]. However, studies on sulfur doped carbons are limited. Poly(sodium 4-styrene sulfonate) [18], poly[(2-hydroxymethyl)thiophene] [12] like polymer materials have been used to produce porous carbons. A molecular precursor that has high sulfur and oxygen content may provide high heteroatom doping and sufficient porosity. In addition, presence of $-SO_3H$ like groups in a precursor may allow cross-linking ability and this property may help to introduce surfur atoms in carbon framework [19]. TsOH contains $-SO_3H$ group in its structure. Sulfur and oxygen constitutes ~18 wt% and 28wt% of TsOH, respectively. In this regard, TsOH was chosen as a molecular starting material in this study because of its high heteroatom content.

In this study, a novel combination of TsOH and $MgCl_2$ were used as precursor and salt template for the synthesis of a carbon material, respectively. Porous carbon materials were synthesized using p-toluenesulfonic acid (TsOH) with and without presence of $MgCl_2.6H_2O$. The synthesized carbons were evaluated in terms of CO_2 capture performance, textural properties, surface chemical stucture and morphology. During pore size evaluation, different DFT (Density functional theory) methods were used for the pore size distribution calculations, and the results were elucidated to determine the drawbacks of using particular method. It was found that $MgCl_2$ templating does not influence ultramicroporosity development, but it helps to increase supermicropore and macropore volumes. CO_2 uptake capacity at flue gas conditions dwindles with salt templating. The material has an interconnected porous network and high heteroatom (sulfur and oxygen) content on its surface. It is believed that investigation of the properties of carbons synthesized by this method may speed up the development of effective porous carbon materials.

2. MATERIALS AND METHODS

2.1. Materials

The p-toluenesulfonic acid monohydrate and Hydrochloric acid (HCl) (37%) were purchased from Merck. Magnesium chloride hexahydrate ($MgCl_2.6H_2O$) was purchased from Sigma-Aldrich. The raw materials were used without any purification.

2.2. Materials Synthesis

In a typical method of TsOH-C synthesis, TsOH was put in alumina crucible, and placed in middle position of alumina tube in a furnace. It was kept for 1 h at 750 °C with heating and cooling rate of 8 °C min^{-1} under Argon atmosphere with flow rate of 1 L min^{-1}. The sample allowed to cool under inert atmosphere until the temperature reaches to 150 °C. The synthesized black carbon product was ground and washed with distilled water and dried at 80 °C overnight in vacuum oven. For the preparation of TsOH-STC, TsOH and $MgCl_2.6H_2O$ were mixed with a weight ratio of 1/16 in deionized water. The water in the solution was allowed to evaporate at 80 °C for at least 6 h in a beaker placed in oil bath. The dried composite powder was ground. The ground powder sample was subjected to pyrolysis in alumina crucible. Pyrolysis conditions implemented on TsOH was also employed on composite powder. The product was washed with

0.25 M HCl to remove inorganic substances. Finally, the powder was washed with distilled water and dried at 80 °C overnight in vacuum oven.

2.3. Materials Characterization

All adsorption isotherms were acquired by using surface area and porosity analyzer ASAP 2020 manufactured by Micromeritics Instruments Corp. N_2 adsorption data were taken at 77 K, while CO_2 data were acquired at 273 K. CO_2 and N_2 adsorption isotherms were obtained at 298 K between 0.01 bar and 1 bar as well. Before the adsorption experiments, the samples were degassed at 250 °C. Helium method was separately performed before each cryogenic nitrogen adsorption experiment. Then the samples were degassed at 100 °C again and finally full isotherms were obtained by using already known dead space values.

Pore size distribution was determined by fitting N_2 adsorption isotherm with DFT model supplied by Micromeritics software designed for slit shape pores on carbon. Brunauer-Emmett-Teller (BET) surface area was calculated using appropriate region on N_2 adsorption isotherm considering that the materials are microporous. Fitting of CO_2 adsorption isotherms were carried out by using NLDFT (non-local density function theory) and DFT models provided by Quantachrome and Micromeritics, respectively. Both pore models were designed for slit shape pores on carbon. IAST selectivity was employed to estimate CO_2 selectivity over N_2. Mole fraction for CO_2/N_2 was selected as 0.15/0.85 at 1 bar (flue gas pressure). IAST is a prediction of adsorption equilibria carried out by using single component adsorption isotherms [20,21]. To carry out the selectivity calculations a Python code (Pyiast) was used [22]. Isosteric heats of adsorption (Q_{st}) were calculated by making use of CO_2 adsorption isotherms obtained at 273 K and 298 K. Scanning electron microscope (SEM) images were obtained with Zeiss Evo LS10. Energy dispersive X-ray spectroscopy (EDS) studies were performed by using Edax-Element EDS detector. ATR-FTIR (Attenuated total reflection-Fourier transform infrared absorption spectroscopy) analyses were performed on Perkin Elmer Spectrum 100. Diamond/Zinc selenide ATR was utilized for the characterization of powdered carbon samples. Each spectrum was acquired with 50 scans while using 4 cm^{-1} resolution between wavenumbers of 4000-650 cm^{-1}. Only fingerprint regions of spectra were provided (1700 cm^{-1} and 650 cm^{-1}) in the article. Because peaks related to carbons were present in this region. Elemental analyses and chemical states of elements were analyzed by Thermo K-Alpha XPS system. Energy calibration was not implemented using C1s peak since there is controversy on referencing of C1s peaks [23]. Photoemission survey spectra were acquired using 100 eV pass energy. On the other hand, pass energy setting for high resolution spectra was 100 eV. CasaXPS software was used to deconvolute high resolution XPS spectra.

3. RESULTS AND DISCUSSION

Synthesis steps of TsOH-STC is shown in Figure 1. The reason behind choosing $MgCl_2.6H_2O$ is explained as follows: $MgCl_2$ melts at 714 °C, which is close to pyrolysis temperatures of carbons. However, $MgCl_2.6H_2O$ has a melting point of 117 °C [14]. Because of its low melting point, it was used as a solvent to homogenously polymerize and carbonize organic compounds [14]. Therefore, a high salt to organic compound ratio (16) was used to benefit from the possible solvent-like effect of $MgCl_2.6H_2O$ to enable homogenous carbonization of TsOH. In this respect, effect of high salt content was investigated on pore development and size distribution.

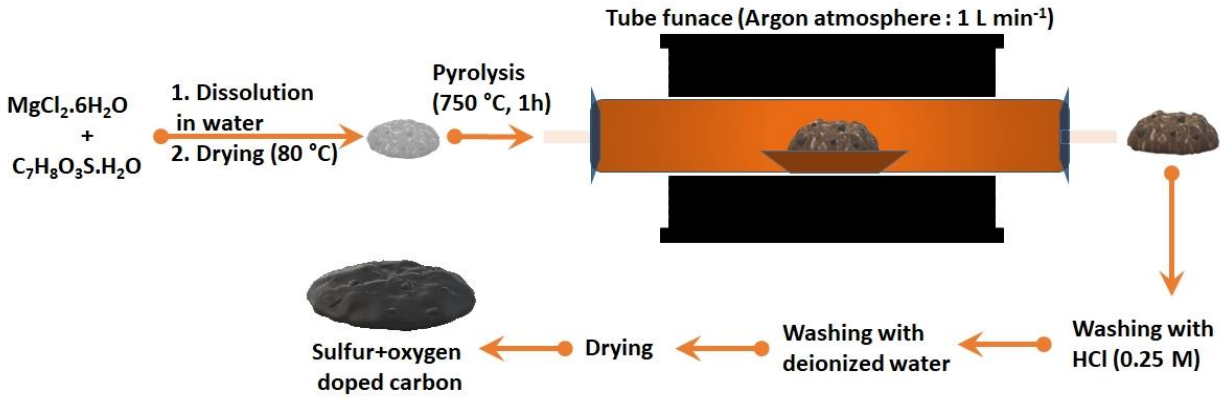

Figure 1. *Synthesis steps of TsOH-STC. Salt to organic compound weight ratio was 16*

Optical images of acid-salt mixture before and after pyrolysis are shown in Figure 2a and b, respectively. As can be seen from the image, the structure is not homogenous. This is mainly because of the excess $MgCl_2$ in the reaction mixture. Figure 2c and d are backscattered electron image and EDS map of the mixture before pyrolysis, which imply that at least homogenous mixing of Mg and Cl elements is attained at macroscopic level (100x). All the sulfonic acid groups in TsOH were ion exchanged, which led to homogeneous dispersion of Mg ions, excess Mg should have clustered as $MgCl_2$. The aim of providing ion exchange on functional groups is as follows: As in the the study of Liu et al., where they used hydrochar material to produce activated carbons, homogenous ultramicropore evolution was obtained by ion exchange generated on -COOH groups on hydrochar using KOH activator [5]. So they postulated that presence of -COOK groups provide activation effect.

Figure 2e is secondary electron image of TsOH-STC. Figure 2f, g, h, i and j are EDS maps of TsOH-STC. EDS analysis revealed that bipyramid shaped particles are MgO (They are composed of oxygen and magnesium). There is no monomodal size distribution of MgO particles. Except MgO, the structure contains sulfur and carbon.

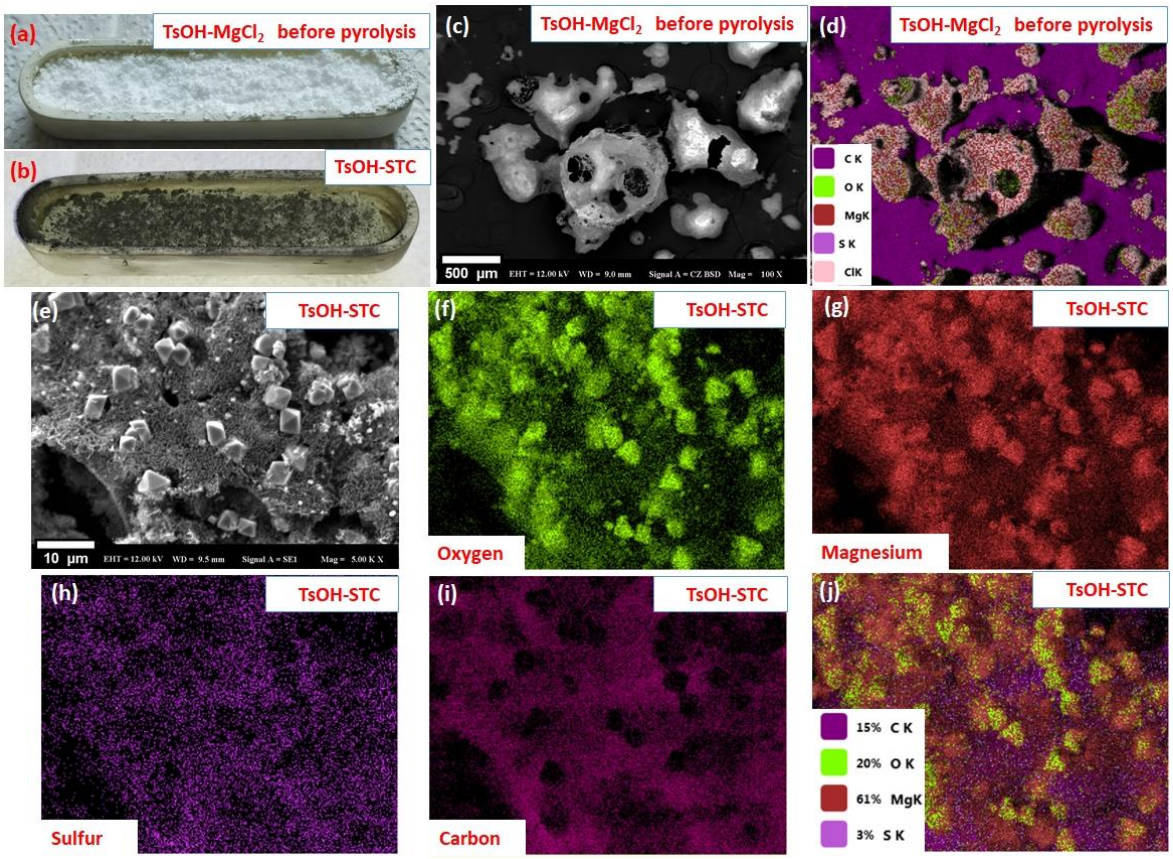

Figure 2. *(a) Optical image of TsOH and $MgCl_2.6H_2O$ mixture before pyrolysis, (b) is optical image of TsOH-STC after pyrolysis, (c) and (d) are backscattered electron image of TsOH/$MgCl_2$ mixture before pyrolysis and EDS map, respectively. (e), (f), (g), (h), (i) and (j) are secondary electron image of TsOH-STC, oxygen, magnesium, sulfur, carbon and overlay EDS maps of major elements detected, respectively*

Figure 3 shows scanning electron microscopy images of rinsed samples, the insets are tables related to composition of samples obtained by EDS. Micrographs of TsOH-C are shown in Figure 3a, b and c. The images reveal that the TsOH-C has no large pores and it is densley packed. In terms of elemental composition, one notable property of TsOH-C is its low oxygen (O) content, which is around 1 wt%. Sulfur content is ~11 wt%. It was assumed that presence of sulfur may provide high energy adsorption sites for CO_2 molecules. Because sulfur has lone pairs of electrons. Therefore, sulfur may act as Lewis base and consequently, may provide basicity on carbon surface. However, it should be noted that thiophene type functionalities and oxidized sulfur groups such as sulfoxides are known to positively influence CO_2 adsorption [24]. Not all type of sulfur functionalities have role on adsorption of CO_2 [24].

Figure 3d, e and f are micrographs of TsOH-STC. TsOH-STC has interconnected 3D porous framework unlike TsOH-C as a result of $MgCl_2$ templating. The structure contain holes having sizes between 500 nm and 800 nm as indicated by red arrows (Figure 3d). During the replication process of salt crystals sheet-like morphology emerged as indicated by yellow arrow in Figure 3e. Thickness values of sheets are beyond measurable limit of used SEM. However, the layer thicknesses were assumed to be around 100 nm or less.

TsOH-STC is mostly composed of 3D porous network as explained above, on the other hand, dense regions are present as well (Figure 3f). This implies that there is inhomogeneity in terms of morphology. This inhomogeneity is believed to be arising from the drying conditions implemented (freeze drying may be a relavant alternative) and high heating rate (8 °C min^{-1}). To get over that problem lower heating rates can be used to provide time for TsOH and $MgCl_2$ to melt and homogenously mix. Inset in Figure 3f represents the elemental distribution of TsOH-STC. After acid washing almost all Mg was successfully removed. There is a slight silicon contamination, which is believed to be contamination from silicon oil used during drying process. Sulfur content is on the level of 12 wt%. This value is almost the same as that of TsOH-C. The

only significant difference between TsOH-C and TsOH-STC is oxygen content. TsOH-STC has around 4 times higher oxygen (4 wt %) than TsOH-C in the bulk.

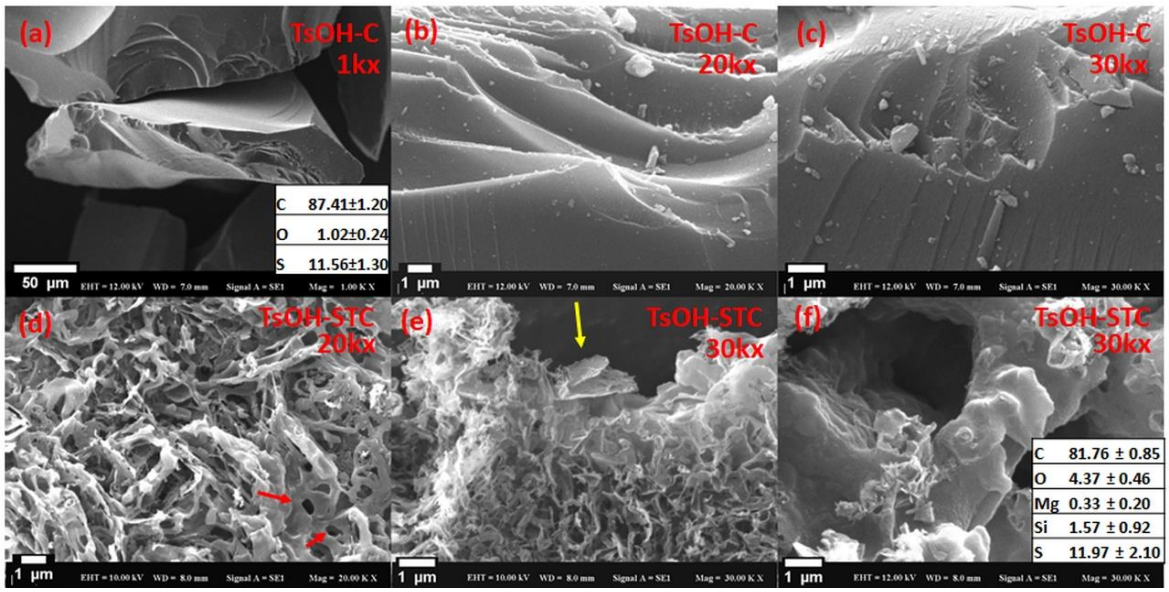

Figure 3. *(a), (b) and (c) are SEM image of TsOH, (d), (e) and (d) are SEM image of TsOH-STC. Insets in (a) and (e) are weight concentrations of elements*

In order to corroborate the chemical structural information obtained by using EDS, ATR-FTIR analyses were also performed. Figure 4 shows ATR-FTIR spectra of synthesized carbons. Since prominent bands are located in the fingerprint region, the spectra were drawn between 1700-650 cm^{-1} rather than 4000 cm^{-1} and 650 cm^{-1}. Expectedly, IR spectra is subtle due to high carbonization temperature. Namely, carbonization eliminated most of the functional groups and induced drastic structural changes on organic molecule. The peak at 1540 cm^{-1} was assigned to aromatic ring stretching (C=C). The band at 1120 cm^{-1} corresponds to C-O stretching. Both absorption bands are present in carbons with varying intensities. TsOH-C has significantly lower C-O stretching band. This result is in correlation with the fact that TsOH-STC has significantly higher oxygen (EDS) than TsOH-C. However, one should also be sceptical about comparison of concentration of functional groups based on peak intensities between different spectra. Because carbons has high absorption of infrared radiation and diamond/ZnSe ATR is not ideal for black samples like carbons.

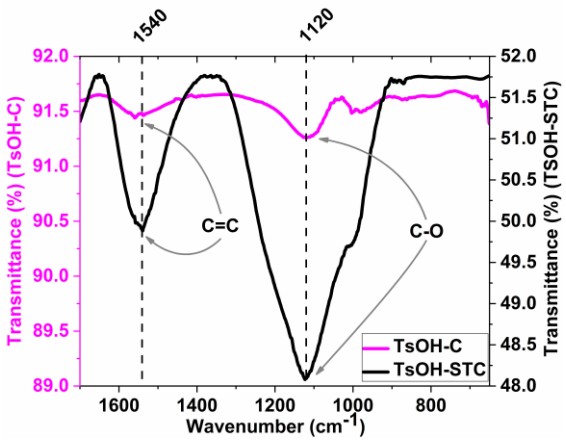

Figure 4. *a) ATR-FTIR spectra of TsOH-C and TsOH-STC*

Adsorption processes or chemical reactions take place on surfaces. Therefore, a surface sensitive technique, XPS was used to investigate elemental composition and chemical state of the elements (Figure 5). Figure 5a and d show XPS survey spectra of TsOH-C and TsOH-STC. C1s and O1s and S2p peaks are highlighted.

Quantifications results are also provided. There is substantial difference between quantification results obtained by means of EDS and XPS for TsOH-C (Figure 5a). Namely, oxygen constitutes 1 wt% of TsOH-C in terms of EDS, but XPS results reveal that oxygen content is 7.87 at% (9.69 wt%). The underlying cause for this is explained as follows: XPS is surface sensitive technique. However, EDS measures the bulk because high energy electron beam penetrates deep inside the material and interaction volume of X-rays is large.

Pyrolysis at elevetated temperatures (750 °C) ensures that temperature sensitive functional groups are removed such as sulfoxides or sulfonic acids [25]. However, it seems that after exposure to air, carbon samples acquired oxidized sulfur functional groups. This result is in agreement with literature because oxidized sulfur was also observed on carbons derived from sulfur bearing polymers (carbons pyrolized under nitrogen at 800 °C) [26]. Considering TsOH-STC, elemental composition is also different compared to EDS results. Salt temlating decreased surface oxygen, but sulfur content remained similar (Figure 5d). Figure 5b and e are deconvolution of the core energy level spectra of S 2p of carbons. S 2p peaks of TsOH-C and TsOH-STC consist of 4 and 3 components, respectively. Two peaks at 164 eV and 165 eV are related to C-S functional group in thiophene-S [27] or C=S [28]. The peaks at 166 eV and 167 eV are ascribed to oxidized sulfur/sulfoxides [16,25] in TsOH-C and TsOH-STC. Oxidized sulfur functionalities constitute 18.2% of sulfur functionalities in TsOH-C and that of TsOH-STC is 22.3%. However, TsOH-C has more oxygen on its surface than TsOH-STC, which should present as C-O like functional groups. This results implies that TsOH-C has slightly more polar surface than TsOH-STC. C 1s core level spectra were also acquired (Figure 5c and f). Electronegativity of carbon is similar to that of sulfur. So binding energy of peak related to C-S should be at similar position to C-C bonds. In that sense, the peaks at 284.8 eV may be ascribed to C-C bond [29] and C-S bond [24]. The peaks at 285.8 eV is related to ether (C-O) [30] or C-S bond [29]. Overall, in terms of C 1s spectra, there is no significant difference between carbons` oxidation states.

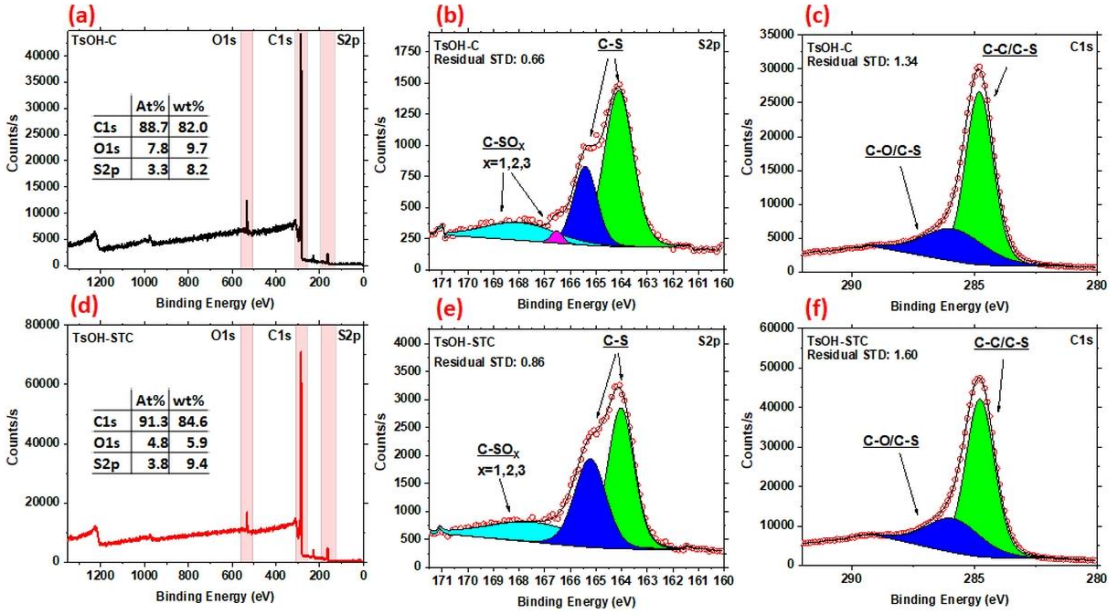

Figure 5. *a) and d) are XPS survey spectra of TsOH-C and TsOH-STC. b) and e) are deconvoluted S 2p core level spectra. c) and f) are deconvoluted C 1s spectra (Residual standard deviation: Residual STD)*

Nitrogen adsorption-desorption isotherm of TsOH-STC has H3 type hysteresis loop based on classification by IUPAC (International Union of Pure and Applied Chemistry) as shown in Figure 6a and its inset. The steep slope at low relative pressures (<0.01 P/P_0) suggests that narrow microporosity is present, i.e., ultramicropores (<0.7 nm), which are no bigger than 2-3 molecular diameters of adsorptive gas [31]. There is no leveling off at high relative pressures, which dictates that macropores are present and they are not filled at atmospheric pressure [31]. DFT differential pore size distribution (PSD) and cumulative pore volume (CPV) graphs are shown in Figure 6b. It is revealed that the carbon material has hierarchical

porosity. This structure is beneficial for some applications, in which macropores and mesopores enable accessibility to microporosity. BET surface area of TsOH-STC is 712.60 m^2 g^{-1} (Table 1). That of DFT estimation is 591.36 m^2 g^{-1}. It should be noted that BET underestimates the surface area in the case of microporous materials and overestimates for materials having wide pores [32]. However, DFT calculation yielded lower specific surface area value, which means that though micropores are present, presence of hierarchical pore structure complicates surface area determination and comparison of results of different methods.

TsOH-C possesses an unusual nitrogen adsorption isotherm (Figure 6c). Kinetic restrictions is believed to produce this unrealistic isotherm. Probably, TsOH-C is composed of interconnected micropores, and has bottle-neck type pores. Time taken between adoption points also corroborates the idea that the material conveys a molecular sieving effect for N_2 molecules at cryogenic temperatures (Figure 6d). Because N_2 adsorption time for TsOH-STC is significantly lower than TsOH due to hierarchical pore structure, which facilitates diffusion of adsorbate molecules. Low pressure hysteresis behavior reinforces this assumption, which is a common phenomenon observed particularly in microporous polymers that is the result of ill-connected micropores [33]. Considering the adsorption isotherm shape of TsOH-C, it resembles type I(a) isotherm according to IUPAC classification, which is an indication of presence of narrow micropore size distribution. This assumption seems plausible. Because in the following sections, it will be seen that material is composed of narrow micropores (CO_2 adsorption isotherms related DFT estimation). The difference arising between TsOH-C and TsOH-STC is the absence of mesoporosity and macroporosity (external surface) in the former one. As it was mentioned, these wide pores facilitate access to microspores. Due to kinetic restrictions, the TsOH-C isotherm obtained is not at equilibrium and prone to give false textural information as BET surface area was calculated to be 224.65 m^2 g^{-1}.

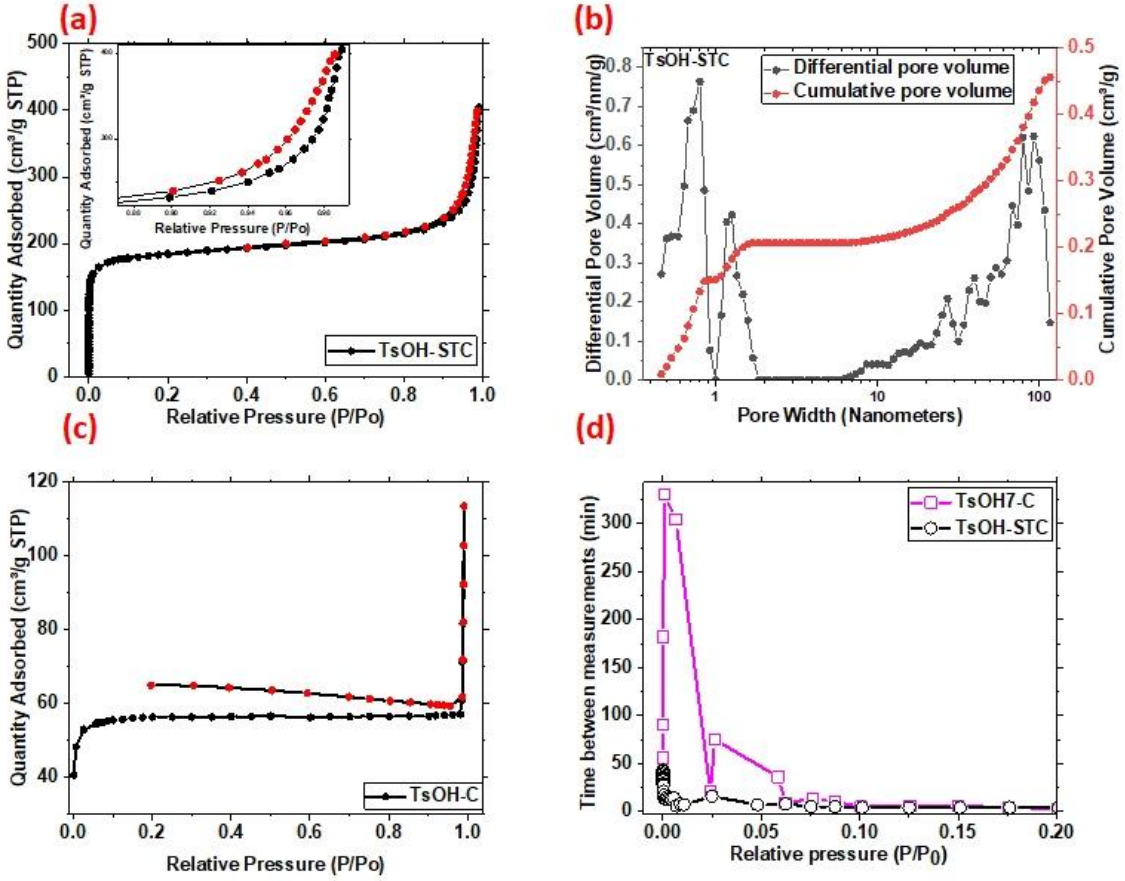

Figure 6. *(a) N_2 adsorption-desorption isotherm of TsOH-STC at 77 K, inset is hysteresis region of the same isotherm. (b) PSD and CPV distributions for TsOH-STC based on DFT method. (c) N_2 adsorption-desorption isotherm of TsOH-C at 77 K. (d) Time taken between adsorption points with cryogenic N_2*

More trials were implemented on TsOH-C. Sample was also subjected to degassing at 250 °C instead of 200 °C, to see the effect of degassing on adsorption. Cryogenic N_2 adsorption equilibrium was attained at extremely slowly (equlibrium time was considerably slower than that obtained by using the sample degassed at 200 °C while all the other experimental parameters were same) for that sample. In addition, sample mass has an influence on measurement time. In this context, there was also trials with dwindling the sample mass to decrease measurement time. There was negligible influence of mass of the adsorbent on adsorption time with selected experimental conditions. Overall, it is not feasible to utilize cryogenic N_2 adsorption for these type of benzene derivative carbons. Because it is a well-known phenomenon in literature that though N_2 is the most widely used adsorbate, completion of measurements dictates duration for more than 100 h when pore sizes approaches to the adsorbate molecule size [34]. O_2, Ar and CO_2 adsorption options are more feasible. It is believed that TsOH derived carbons have so small pores probably with interconnected nature that they have a sieving effect for nitrogen molecules at cryogenic temperatures.

Table 1. *Textural properties of TsOH-STC*

N_2 adsorption at 77 K (Material: TsOH-STC)				
BET surface area ($m^2\ g^{-1}$)	DFT method surface area ($m^2\ g^{-1}$)	Total pore volume (cm^3/g) (DFT method) (<=117 nm)	Micropore volume below 0.7 nm (cm^3/g) (DFT method)	Micropore volume below 1 nm (cm^3/g) (DFT method
712	591	0.46	0.1	0.15

Nitrogen adsorption is complemented with CO_2 adsorption at 273 K as shown in Figure 7a. Up until reaching the crossover at 0.35 bar, TsOH-C showed slightly higher CO_2 uptake. This is an indication of slightly higher content of smallest micropores for this sample. However, at high pressures TsOH-STC absorbs higher quantities of CO_2. In addition, concave shape of CO_2 adsorption isotherms is an indication of strong adsorption potential [32]. DFT model on carbon with slit shape pores was used to fit experimental data, which is obtained from Micromeritics' DFT library. CPV and PSD are shown in Figure 7b. Interestingly, there is a discrepancy between uptake behavior of experimental isotherms and DFT derived pore size and volume information. Throughout the pore size range TsOH-C performs better in CPV graphs, but TsOH-STC is superior to TsOH-C beyond 0.35 bar in the experimental isotherm. The attained pore volumes at 1 nm by CO_2 adsorption at 273 K are 0.09 $cm^3\ g^{-1}$ for TsOH-STC and 0.1 $cm^3\ g^{-1}$ for TsOH-C as shown in Table 2. N_2 adsorption related calculations yielded different pore volume information, i.e., pore volume below 1 nm is 0.15 $cm^3\ g^{-1}$ for TsOH-STC with cryogenic nitrogen adsorption. To elucidate the discrepancy, NLDFT method (for CO_2 on carbon at 273 K) from Quantachrome DFT library was also used (Figure 7c). Contrary to DFT method, NLDFT method follows the trend of the experimental isotherms. Namely, TsOH-C has slightly higher CPV at smallest pores and beyond around 0.6 nm TsOH-STC performs better than TsOH-C. Total pore volume of samples at 0.82 nm (measurable limit) are 0.17 $cm^3\ g^{-1}$ for TsOH-STC and 0.15 $cm^3\ g^{-1}$ for TsOH-C according to NLDFT, which also correlates with N_2 adsorption related DFT result (see Figure 6b, Tables 1, 2). Considering PSD, two methods yield comparable results. Ultramicropores in the range of 0.5-0.6 nm are common for both with small shift to lower values for TsOH-C, and there is an increasing trend beyond 0.7 nm up to 0.82 nm in CPV graph. NLDFT related method ends at 0.82 nm. However, DFT method enables reaching slightly above 0.9 nm.

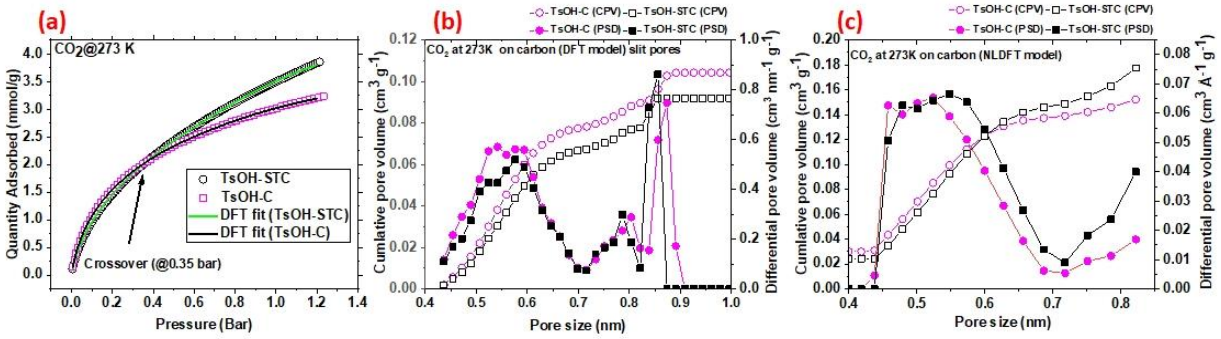

Figure 7. *(a) Experimental CO_2 adsorption isotherms of samples at 273 K and DFT fits of corresponding isotherms, (b) CPV and PSD versus pore width based on DFT calculation for slit like pores (Micromeritics library), (c) CPV and PSD versus pore width based on NLDFT model calculation (Quantachrome library)*

As mentioned above, cryogenic nitrogen adsorption is not suitable for TsOH-C. Because N_2 has a quadruple moment and this can cause specific interactions on adsorbent surface [32] along with other possible limitations. Namely, it can take very long time for N_2 molecules to diffuse into the pores at cryogenic tempratures in narrow pores. On the contrary, CO_2 adsorption can be obtained more easily due to enhanced adsorption kinetics. Because CO_2 adsorption takes place at 273 K. High temperature facilitates diffusion. It is possible for CO_2 to enter smallest pores due to mitigated kinetic restrictions, though CO_2 molecule has a higher quadruple moment than N_2. Table 2 shows surface area values calculated based on CO_2-DFT and CO_2-NLDFT methods for carbon. Those of TsOH-C is 526 m^2 g^{-1} and 672 m^2 g^{-1} for TsOH-STC based on CO_2-DFT model. Considering CO_2-NLDFT results, TsOH-STC has a surface area of 665 m^2 g^{-1}, which is close to DFT method's result. However, that of TsOH-C is 614 m^2 g^{-1}, which is 88 m^2 g^{-1} higher than DFT result based surface area. Overall, based on the obtained results, it is speculated that as expectedly NLDFT method gives more plausible textural information than DFT for the studied carbons.

It should be noted that there is a discrepancy between micropore volumes found with N_2 adsorption interpretation and CO_2 adsorption interpretation for TsOH-STC. It should be emphasized that the two calculation methods are different, one is DFT and the other one is NLDFT. Besides, CO_2 gas is more polar than N_2, which may mean that even at 273 K, CO_2 molecules pack more densely in ultramicropores of a polar material due to higher adsorption tendency.

Table 2. *Textural properties of synthesized samples*

CO_2 adsorption at 0 °C	DFT model: Micropore volume <= 1 nm (cm^3 g^{-1})	NLDFT model: Micropore volume <= 0.82 nm (cm^3 g^{-1})	DFT model: Micropore volume <= 0.7 nm (cm^3 g^{-1})	NLDFT model: Micropore volume <= 0.7 nm (cm^3 g^{-1})	DFT model: Micropore surface area (m^2 g^{-1})	NLDFT model: Micropore surface area (m^2 g^{-1}) (<= 0.82 nm)
TsOH-STC	0.09	0.17	0.06	0.15	672	665
TsOH-C	0.10	0.15	0.08	0.14	526	614
CO_2 adsorption at 25 °C	CO_2 uptake at 0.15 bar (mmol g^{-1})	CO_2 uptake at 1 bar (mmol g^{-1})	N_2 uptake at 0.15 bar (mmol g^{-1})	N_2 uptake at 1 bar (mmol g^{-1})	CO_2/N_2 Selectivity at 1 bar (CO_2/N_2:0.15/0.85)	Isosteric heat of adsorption at 0.1 mmol g^{-1}
TsOH-STC	0.67	2.47	0.06	0.33	13.5	25
TsOH-C	0.78	2.21	0.05	0.32	19.7	23

During post-combustion carbon capture processes flue gas is composed of mostly nitrogen and CO_2. The percentage of CO_2 in flue gas is between 3 and 15 % [35] and nitrogen content is around 70 % [36]. Flue gas is at atmospheric pressure and its temperature is in the range of 320 K and 400 K [1]. In this context, for the sake of understanding functionality of carbons for CO_2 capture purposes, CO_2 and N_2 adsorption isotherms were obtained at 298 K (Figure 8a). Performance values are tabulated in Table 2. CO_2 uptakes (@0.15 bar) are 0.67 mmol g^{-1} and 0.78 mmol g^{-1} for TsOH-STC and TsOH-C, respectively. CO_2 uptake values (at 0.15 bar) can be considered moderate because as high as 1.90 mmol g^{-1} was reached with polyacrylonitrile derived KOH activated carbons [37]. In that study, nitrogen doping enabled high CO_2 affinity of carbon surface and KOH activation provided porosity. At higher pressures like 1 bar, TsOH-STC is superior. It reached a gas uptake value of 2.47 mmol g^{-1}, which is 0.26 mmol g^{-1} higher than that of TsOH-C. The difference is not remarkable, which is the result of effective pore size range for CO_2 adsorption. It is known that due to enhanced adsorption potential, smallest pores in the range of ultramicropores (<0.7 nm) account for noticeable CO_2 adsorption at elevated temperatures and low pressures like 0.15 bar, respectively [11,29,38]. The similar ultamicropore volumes (0.15 cm^3 g^{-1} for TsOH-STC and 0.14 cm^3 g^{-1} for TsOH-C) is reflected in similar uptake performances at 0.15 bar. Isotherms obtained at 273 K overlap at 0.35 bar (up to that point TsOH has slightly higher CO_2 uptake). It yields a overlapping of pore volume plots at around 0.6 nm. Higher uptake performance of TsOH-C at 0.15 bar at 298 K is due to having higher ultramicropore volume at around 0.6 nm. Higher performance at 1 bar for TsOH-STC is ascribed to higher concentration of supermicropores. The higher uptake ability cannot be related to small mesopores. Because TsOH-STC lacks small mesopores as shown in Figure 6b.

Uptake performance is not the only required aspect of a good adsorbent. There will be a competition between different types of gas molecules during adsorption of flue gas mixture. So gas selectivity is an important aspect. IAST selectivity for CO_2/N_2 mixture in the ratio of 0.15:0.85 (total pressure is 1 bar) was calculated based on Equation (1):

$$S_{IAST} = \frac{x_{CO_2} \cdot p_{N_2}}{x_{N_2} \cdot P_{CO_2}} \quad (1)$$

x_{CO2} and x_{N2} are the mole fraction of CO_2 in adsorbed phase, respectively. P_{N2} and P_{CO2} are partial pressures of N_2 and CO_2 in gas mixture, respectively. The selectivities at flue gas conditions (@1 bar, CO_2/N_2:0.15/0.85) are 13.5 for TsOH-STC and 19.7 for TsOH-C (Figure 8b). The selectivity results are lower than some of the values reported in literature [16,39], but especially that of TsOH-C can be comparable with other carbon based adsorbents [13]. Having higher surface area is beneficial for adsorption of competitive gasses like N_2 [24]. Therefore, superior selectivity of TsOH-C may be ascribed to lower surface area and lack of external surface area. Another possibility is surface basicity. If surface chemical structure accounts for higher selectivity, then Q_{st} should correlate with that. Because both processes are related to adsorbent-adsorbate interactions [40].

Q_{st} can serve as a tool to understand the surface properties of the adsorbent, i.e, surface heterogeneity etc., and it was calculated by using Clausius−Clapeyron [41,42] Equation (2):

$$Q_{st} = R \frac{T_1 T_2}{T_2 - T_1} \ln\left(\frac{P_2}{P_1}\right) \quad (2)$$

where T_1 and T_2 are the temperatures of the used isotherms, P_1 and P_2 are pressure values in which same adsorbed amount is attained in corresponding isotherms, and R is gas the constant (8.314 J K^{-1} mol^{-1}). Q_{st} as a function of surface coverage is shown in Figure 8c. At low surface coverages high energy sites are first occupied by CO_2 molecules. Because most favorable sites are occupied firstly [11]. At high surface coverages lateral interactions take place (interaction between CO_2 molecules). At low surface coverages, maximum Q_{st} value for TsOH-STC is 25.7 kJ mol^{-1} and that of TsOH750 is 24.9 kJ mol^{-1}. As the surface coverage increases Q_{st} tends to decrease for TsOH-STC. Generally Q_{st} values tends to gradually decrease as site occupancy increases [24,25]. In the case of synthesized carbons, there is an increasing trend first,

followed by a plateau and decrease. Besides, that of TsOH-C increases at high adsorbed amounts. One of the reasons for the observed behavior is diffusional limitations influencing heat of adsorption [11]. Overall, IAST selectivities differ, but Q_{st} values at low surface coverages are similar. This implies that higher gas selectivity is the result of lack of external surface of TsOH-C. On the contrary, TsOH-STC has more polar surface due to higher oxygen content, which may be reflected in slightly higher Q_{st}. Surface sulfur contents and oxidation states of sulfur species are similar for both carbons. Therefore, no deduction could be put forward on the effect of sulfur on CO_2 adsorption in this study.

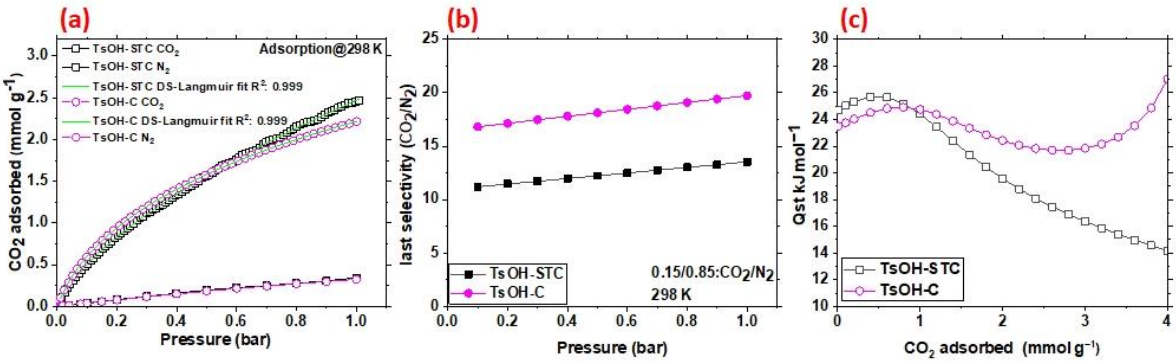

Figure 8. *(a) Adsorption isotherms of samples at 298 K and fitting curves based on dual site Langmuir equation (DS-Langmuir), (b) calculated IAST selectivity for CO_2/N_2 considering CO_2 mole fraction as 0.15 in composite gas, (c) Q_{st} distribution for CO_2 versus surface coverage based on isotherms obtained at 273 K and 298 K*

4. CONCLUSION

In this study, a carbon material with 3D porous architecture was prepared by salt templating. TsOH was used to prepare carbon materials with or without $MgCl_2$ salt template at 750 °C under Argon atmosphere. CO_2 sorption behavior, textural properties, surface chemical structure were evaluated to see the effect of salt templating. XPS and EDS results transpired that heteroatom content in the bulk significantly different than that on the surface. Salt templating decreased oxygen content on the surface, and both samples possess oxidized form of sulfur on the surface. TsOH-C has slightly more polar surface than TsOH-STC by having more C-O like bonds. TsOH-C exhibited N_2-phobic behavior at cryogenic temperatures due to lack of external surface area. On the contrary, salt templating enabled formation of hierarchical pore structure in TsOH-STC. At typical flue gas condition of 0.15 bar (298 K), the uptake values for TsOH-STC and TsOH-C are 0.67 mmol g^{-1} and 0.78 mmol g^{-1}, respectively. At higher pressures like 1 bar, TsOH-STC reaches 2.47 mmol g^{-1}, whereas that of TsOH-C is 2.21 mmol g^{-1}. IAST CO_2:N_2 (0.15/0.85) selectivity of TsOH-C (19.7) is higher than that of TsOH-STC (13.5) at 1 bar. However, Q_{st} values for carbons are similar: 25.7 kJ mol^{-1} for TsOH-STC and 24.9 kJ mol^{-1} for TsOH750 at low surface coverages. $MgCl_2$ salt templated synthesis lowers the gas selectivity, but does not influence CO_2 binding energy on high energy active sites. Higher gas selectivity is the result of narrow PSD and lack of external surface of TsOH-C. TsOH-C has more polar surface due to higher oxygen content, which may be reflected in slightly higher Q_{st}. Surface sulfur and types of sulfur species are similar for both carbons. Therefore, no deduction could be put forward on the effect of sulfur on CO_2 adsorption in this study. Besides, it was also understood from this study that it is not enough to choose DFT calculation method used in adsorption that provides the least fitting error. There should also be an evaluation between experimental and calculated isotherms of different materials for a better understanding.

ACKNOWLEDGEMENTS

This research did not receive any specific grant from funding agencies in the public, commercial, or not-for-profit sectors. Author thanks the anonymous reviewers for their constructive suggestions. Author would like to thank Richard T. Haasch for his help on CasaXPS software studies.

CONFLICTS OF INTEREST

No conflict of interest was declared by the author.

REFERENCES

[1] Songolzadeh, M., Soleimani, M., Takht Ravanchi, M., Songolzadeh, R., "Carbon dioxide separation from flue gases: A technological review emphasizing reduction in greenhouse gas emissions", The Scientific World Journal, 2014: 1-34, (2014).

[2] Zhang, J., Xiao, P., Li, G., Webley, P.A., "Effect of flue gas impurities on CO_2 capture performance from flue gas at coal-fired power stations by vacuum swing adsorption", Energy Procedia, 1: 1115–1122, (2009).

[3] Ramezanipour Penchah, H., Ghaemi, A., Ganadzadeh Gilani, H., "Benzene-Based Hyper-Cross-Linked Polymer with Enhanced Adsorption Capacity for CO_2 Capture", Energy and Fuels, 33(12): 12578-12586, (2019).

[4] Armutlulu, A., Naeem, M.A., Liu, H.J., Kim, S.M., Kierzkowska, A., Fedorov, A., Müller, C.R., "Multishelled CaO Microspheres Stabilized by Atomic Layer Deposition of Al_2O_3 for Enhanced CO_2 Capture Performance", Advanced Materials, (29): 1–9, (2017).

[5] Liu, Z., Zhang, Z., Jia, Z., Zhao, L., Zhang, T., Xing, W., Komarneni, S., Subhan, F., Yan Z., "New strategy to prepare ultramicroporous carbon by ionic activation for superior CO_2 capture", Chemical Engineering Journal, 337: 290–299, (2018).

[6] Wang, R., Mi, J.S., Dong, X.Y., Liu, X.F., Lv, Y.R., Du, J., Zhao, J.Y., Zang, S.Q., "Creating a Polar Surface in Carbon Frameworks from Single-Source Metal-Organic Frameworks for Advanced CO_2 Uptake and Lithium-Sulfur Batteries" Chemistry of Materials, 31: 4258–4266, (2019).

[7] Xu, F., Wu, D., Fu, R., Wei, B., "Design and preparation of porous carbons from conjugated polymer precursors", Materials Today, 20: 629–656, (2017).

[8] Pardakhti, M., Jafari, T., Tobin, Z., Dutta, B., Moharreri, E., Shemshaki, N.S., Suib, S., Srivastava, R., "Trends in Solid Adsorbent Materials Development for CO_2 Capture", Applied Materials and Interfaces, 11: 34533–34559, (2019).

[9] Nwodika, C., Onukwuli, O.D., "Adsorption Study of Kinetics and Equilibrium of Basic Dye on Kola Nut Pod Carbon", Gazi University Journal of Science, 30, 86–102, (2017).

[10] Altuntaş, D. B., Aslan, S., Nevruzoğlu, V., "Carbon Microrod Material Derived From Human Hair and Its Electrochemical Supercapacitor Application", Gazi University Journal of Science, 34(3): 695-708, (2021). DOI: https://doi.org/10.35378/gujs.712032

[11] Sethia, G., Sayari, A., "Comprehensive study of ultra-microporous nitrogen-doped activated carbon for CO_2 capture", Carbon, 93: 68–80, (2015).

[12] Hwang, C.C., Tour, J.J., Kittrell, C., Espinal, L., Alemany, L.B., Tour, J.M., "Capturing carbon dioxide as a polymer from natural gas", Nature Communications, 5: 1–7, (2014).

[13] Shi, J., Yan, N., Cui, H., Xu, J., Liu, Y., Zhang, S., "Salt Template Synthesis of Nitrogen and Sulfur Co-Doped Porous Carbons as CO_2 Adsorbents", ACS Sustainable Chemistry and Engineering, 7: 19513–19521, (2019).

[14] Pampel, J., Mehmood, A., Antonietti, M.,. Fellinger, T.P, "Ionothermal template transformations for preparation of tubular porous nitrogen doped carbons", Materials Horizons, 4: 493–501, (2017).

[15] Wang, M., Fan, X., Zhang, L., Liu, J., Wang, B., Cheng, R., Li, M., Tian, J., Shi, J., "Probing the role of O-containing groups in CO_2 adsorption of N-doped porous activated carbon", Nanoscale, 9: 17593–17600, (2017).

[16] Rao, L., Ma, R., Liu, S., Wang, L., Wu, Z., Yang, J., Hu, X., "Nitrogen enriched porous carbons from D-glucose with excellent CO_2 capture performance", Chemical Engineering Journal, 362: 794–801, (2019).

[17] Wang, E.J., Sui, Z.Y., Sun, Y.N., Ma, Z., Han, B.H., "Effect of Porosity Parameters and Surface Chemistry on Carbon Dioxide Adsorption in Sulfur-Doped Porous Carbons", Langmuir, 34: 6358–6366, (2018).

[18] Seredych, M., Jagiello, J., Bandosz, T.J., "Complexity of CO_2 adsorption on nanoporous sulfur-doped carbons - Is surface chemistry an important factor?", Carbon, 74: 207–217, (2014).

[19] Sun, Y., Zhao, J., Wang, J., Tang, N., Zhao, R., Zhang, D., Guan, T., Li K., "Sulfur-Doped Millimeter-Sized Microporous Activated Carbon Spheres Derived from Sulfonated Poly(styrene-divinylbenzene) for CO_2 Capture", The Journal of Physical Chemistry C, 121: 10000–10009, (2017).

[20] Myers, A.L., Prausnitz, J.M., "Thermodynamics of mixed-gas adsorption", AIChE Journal, 11: 121–127, (1965).

[21] Nicolae, S.A., Szilágyi, P.Á., Titirici, M.M., "Soft templating production of porous carbon adsorbents for CO_2 and H_2S capture", Carbon, 169: 193–204, (2020).

[22] Simon, C.M., Smit, B., Haranczyk M., "PyIAST: Ideal adsorbed solution theory (IAST) Python package", Computer Physics Communications, 200: 364–380, (2016).

[23] Greczynski, G., Hultman, L., "X-ray photoelectron spectroscopy: Towards reliable binding energy referencing", Progress in Materials Science, 107: 100591, (2020).

[24] Saha, D., Kienbaum, M.J., "Role of oxygen, nitrogen and sulfur functionalities on the surface of nanoporous carbons in CO_2 adsorption: A critical review", Microporous Mesoporous Materials, 287: 29–55, (2019).

[25] Zaman, A.C., "Polyol derived sulfonated solvothermal carbon for efficient dye removal from aqueous solutions", Journal of Molecular Liquids, 249: 892–903, (2018).

[26] Seredych, M., Rodríguez-Castellón, E., Bandosz, T.J., "Alterations of S-doped porous carbon-rGO composites surface features upon CO_2 adsorption at ambient conditions", Carbon, 107: 501–509, (2016).

[27] Hu, Y., Yang, J., Tian, J., Jia, L., Yu, J.S., "Waste frying oil as a precursor for one-step synthesis of sulfur-doped carbon dots with pH-sensitive photoluminescence", Carbon, 77: 775–782, (2014).

[28] Qian, W., Sun, F., Xu, Y., Qiu, L., Liu, C., Wang, S., Yan, F., "Human hair-derived carbon flakes for electrochemical supercapacitors", Energy and Environmental Science, 7: 379–386, (2014).

[29] Seema, H., Kemp, K.C., Le, N.H., Park, S.W., Chandra V., Lee J.W., Kim K.S., “Highly selective CO2 capture by S-doped microporous carbon materials”, Carbon, 66: 320–326, (2014).

[30] Sevilla, M., Fuertes, A.B., "Chemical and structural properties of carbonaceous products obtained by hydrothermal carbonization of saccharides", Chemistry, 15(16): 4195–4203, (2009).

[31] Cychosz, K.A., Guillet-Nicolas, R., García-Martínez, J., Thommes, M., "Recent advances in the textural characterization of hierarchically structured nanoporous materials", Chemical Society Reviews, 46: 389–414, (2017).

[32] Grau-Marin, D., Silvestre-Albero, J., Jardim, E.O., Jagiello, J., Betz, W.R., Peña, L.E., "Evaluation of the textural properties of ultramicroporous carbons using experimental and theoretical methods", Carbon, 157:495–505, (2020).

[33] Jeromenok, J., Weber, J., "Restricted access: On the nature of adsorption/desorption hysteresis in amorphous, microporous polymeric materials", Langmuir, 29: 12982–12989, (2013).

[34] Jagiello, J., Ania, C., Parra, J.B., Cook, C., "Dual gas analysis of microporous carbons using 2D-NLDFT heterogeneous surface model and combined adsorption data of N2 and CO2", Carbon, 91: 330–337, (2015).

[35] Oschatz, M., Antonietti, M., "A search for selectivity to enable CO_2 capture with porous adsorbents", Energy and Environmental Science, 11: 57–70, (2018).

[36] Zhou, L., Fan, J., Cui, G., Shang, X., Tang, Q., Wang, J., Fan, M., "Highly efficient and reversible CO_2 adsorption by amine-grafted platelet SBA-15 with expanded pore diameters and short mesochannels", Green Chemistry, 16: 4009–4016, (2014).

[37] Kim, Y.K., Kim, G.M., Lee, J.W., "Highly porous N-doped carbons impregnated with sodium for efficient CO_2 capture", Journal of Materials Chemistry A, 3: 10919–10927, (2015).

[38] Zhang, Z., Zhou, J., Xing, W., Xue, Q., Yan, Z., Zhuo, S., Qiao, S.Z., "Critical role of small micropores in high CO_2 uptake", Physical Chemistry Chemical Physics, 15: 2523–2529, (2013).

[39] Zhao, Y., Liu, X., Yao, K.X., Zhao, L., Han, Y., "Superior Capture of CO_2 Achieved by Introducing Extra-framework Cations into N-doped Microporous Carbon", Chemistry of Material, 24: 4725–4734, (2012).

[40] Sánchez-Sánchez, Á., Suárez-García, F., Martínez-Alonso, A., Tascón, J.M.D., "Influence of porous texture and surface chemistry on the CO_2 adsorption capacity of porous carbons: Acidic and basic site interactions", ACS Applied Materials & Interfaces, 6: 21237–21247, (2014).

[41] Cimino, R.T., Kowalczyk, P., Ravikovitch, P.I., Neimark, A. V. "Determination of Isosteric Heat of Adsorption by Quenched Solid Density Functional Theory", Langmuir, 33: 1769–1779, (2017).

[42] Rouquerol, F., Rouquerol, J., Sing, K., "Thermodynamics of Adsorption at the Gas–Solid Interface, in: Adsorpt. by Powders Porous Solids", Elsevier, 27–50, (1999).

[43] Xia, Y., Zhu, Y., Tang, Y., "Preparation of sulfur-doped microporous carbons for the storage of hydrogen and carbon dioxide", Carbon, 50: 5543–5553, (2012).

[44] Madani, S.H., Sedghi, S., Biggs, M.J., Pendleton, P., "Analysis of Adsorbate-Adsorbate and Adsorbate-Adsorbent Interactions to Decode Isosteric Heats of Gas Adsorption", ChemPhysChem, 16: 3797–3805, (2015).